

A stronomy & Astrophysics manuscript no.
(will be inserted by hand later)

Skym ion Stars

A strophysical motivations and implications

P rashanth Jaikumar¹ and R achid Ouyed²

¹ Theory Group, Physics Division, Argonne National Laboratory, Argonne, IL 60439 USA
e-mail: jaikumar@phy.anl.gov

² Department of Physics and Astronomy, University of Calgary, Calgary, AB T2N 1N4 Canada
e-mail: ouyed@phas.ucalgary.ca

Received/Accepted

Abstract. We study mass-radius relations for compact stars employing an equation of state (EOS) of dense matter based on a Skyrme uid. The zero-temperature mean-field model is based on mesonic excitations, incorporates the scale breaking of QCD, and accommodates baryons (nucleons) which arise as a solitonic configuration of mesonic fields. Stable configurations are obtained for central densities $c = N = 5.0$ where $N = 2.575 \cdot 10^{14} \text{ g/cc}$ is the nuclear saturation density. These Skym ion Stars are mostly uid, with a crust which we describe by the EOS of Baym, Pethick and Sutherland. They appear to have a mass-radius curve quite different from either neutron or quark stars, and provide a suitable description of the heavier mass neutron stars discovered recently due to the inherently stiff EOS. Within the same model, we compute the dominant neutrino emissivity, and determine the cooling behavior of Skym ion stars with a crust.

Key words. skym ions, compact stars, neutrinos

1. Introduction

An oft-stated goal in the study of compact stars (neutron stars or possibly even quark stars) is the determination of the phase of matter in their interior through astronomical observations (Weber 1999, Lattimer 2000, Heiselberg & Pandharipande 2000). An equation of state is used to describe this phase; since it is an input into the equations that describe the structural properties of the star, it can therefore be constrained by stellar mass and radius observations (van Kerkwijk 2001, Lattimer & Prakash 2001, Lattimer & Prakash 2004). The challenge in this field arises, on the one hand, from our lack of theoretical knowledge of the EOS of matter at the highest densities, and on the other hand, from mass and particularly radius determination of compact stars (Haensel 2003, Heiselberg 2001). Despite improved many-body physics of nuclear and neutron matter of relevance to neutron star interiors (Schwenk 2004, Schwenk 2003), and increasingly accurate estimations of mass and radius (Manchester 2004), a number of EOS remain in use, with no definite or universal answer as to which is the best one at supranuclear densities. That being said, theoretical studies of the nuclear equation of state can, to an extent, be gauged for their relative success when confronted against data (particularly,

accurate radius measurements), and we refer the reader to the article by Lattimer & Prakash 2001 (and references therein) for details.

Until recently, timing measurements of radio binary pulsars yielded accurately measured neutron star masses in the range 1.26 to 1.45 M_⊙ (Thorsett and Chakrabarty 1999). Newer observations of binary systems of pulsars and white dwarfs allow for a larger range of masses; for example, the binary component PSR J0751+1807 with 2.2 ± 0.2 M_⊙ within 1% errors (Nice et al. 2003). We also point out the possible confirmation (at 95% confidence) of pulsars with M > 1.68 M_⊙ by Ransom et al. (2005), following the recent detection of 21 millisecond pulsars in the globular cluster Terzan 5, 13 of which are in binaries. These observations of presumably heavier mass neutron stars seem to favor a stiffer equation of state than has been explored in the literature, at least for the central densities that we consider in this work (c = 5.0 N). Intriguingly, it has been shown in Ouyed & Butler (OB 98) that an equation of state based on the solitonic Skyrme model yields quite stiff equations of state and neutron star masses greater than 2M_⊙ for standard radii of 15 km or so (while still obeying causality limits). In this letter, we extend the work done in OB 98 in two main directions. We

construct the equation of state for the Skyrme uid including a finite pion mass (which was previously ignored and could be important) and subsequently determine mass-radius relations for the entire region of hydrostatic stability. We contrast the mass-radius curve with that of neutron and quark stars. We also address neutrino cooling within the same model to obtain a more complete picture of the behaviour of Skyrme ion stars. Taken with comparisons to recent observations of heavy neutron stars, our main goal in this paper is to motivate, analyze and elucidate the consequences of using the Skyrme model as a description of compact star interiors. This paper is organized as follows: In x2, we consider observational hints for large mass neutron stars. In x3, we describe the Skyrme model, its extension to dense matter at nuclear densities and beyond, and obtain an equation of state. In x4, we display the mass-radius curves that are obtained from this EOS, and consider dominant channels for neutrino emission and cooling of the star. Our findings and conclusions are detailed in x5.

2. Observational motivation

We are closing in on neutron stars both observationally (masses and radii) and theoretically (EOS at high density). Observations of X-ray binaries offer the best support for larger masses with values of $1.8 - 2.4M_{\odot}$ (Quaintrell et al, 2003), $2.4 - 0.27M_{\odot}$ (Clark et al, 2002) and $2.0 - 4.3M_{\odot}$ (Shahbaz et al, 2004) being reported. Although these measurements are not as precise as for radio pulsars¹, they seem to hint at the existence of heavy neutron stars.

Such massive NSs are further suggested indirectly by (i) interpretation of some middle-aged cold neutron stars such as the Vela or Geminga pulsars as moderately heavy stars ($1.6M_{\odot}$) based on their thermal history. These calculations, based on models of neutrino cooling of NSs take proton and neutron superfluidity into account (Kaminker et al, 2001); (ii) modeling of neutrino-driven winds from very massive ($M = 2.0M_{\odot}$) and compact ($R = 10 \text{ km}$) neutron stars which reproduced the r-process abundance pattern with reasonable success (Otsuki et al, 2000; Sumiyoshi et al, 2000), due to the short expansion timescale and high entropy that are required to obtain a high neutron-to-seed ratio. However, such a large mass can be criticized from the preponderance of observational data on neutron star mass; (iii) recent studies by Popov & Prokhorov (2005) addressing the issue of existence and formation of massive Skyrme ion stars. They considered different channels for the formation of massive rapidly rotating neutron stars using a population synthesis code to estimate numbers of massive neutron stars on different evolutionary stages, and found that a significant increase in neutron star mass due to accretion is possible for certain values of initial parameters of the binary. They found stars with $M > 2M_{\odot}$ that

¹ We should note that there is only one NS in a binary radio pulsar system, the pulsar J0751+1807 for which a large mass $2.1 - 0.5M_{\odot}$ has been derived (Nico et al 2004).

fit the description of Skyrme ion stars. The authors argued that a significant part of such heavy stars can be observed as millisecond radio pulsars, as X-ray sources in pairs with white dwarfs, and as accreting neutron stars with very low magnetic fields. These massive Skyrme ion star candidates (with the above mentioned observable signatures) can hopefully be tested in the near future; we refer the interested reader to Popov & Prokhorov (2005) for more details.

The evidence for large neutron star masses is still being debated and one awaits confirmation. However, the large masses hinted at above pose a challenge to models of neutron stars based upon modern EOS even as uncertainties are being reduced by improved two- and three-body forces, relativistic effects and many-body calculations (Heiselberg & Pandharipande 2000). Even the stiffer EOS developed so far seems to be facing difficulty in accounting for the extreme values (up to $2.4M_{\odot}$; see discussion in Heiselberg 2001). This brings us to a theoretical discussion of the Skyrme model as an alternative.

3. Theoretical motivation

3.1. The Skyrme model

Well before the discovery of Quantum Chromodynamics (QCD) as the fundamental theory of the strong force, Skyrme (1962) provided a model based on pionic excitations, in which the nucleon arises as a classical configuration of the pion fields with a non-trivial topology and a localized energy density (a soliton). This is remarkable in that it allows us to consider fermions (nucleons) in a bosonic (pionic) theory without introducing any explicit fermion fields. The Skyrme model has been placed on a sound theoretical footing in subsequent analyses (Witten 1979) and it is now accepted as a valid description for certain aspects of the strong force. Its connection to phenomenological nuclear forces is well established (Nyman and Riska 1990), and its justification based on large N_c arguments ('t Hooft 1974) stemming from a quark-gluon picture indicates that it acts as a 'bridge' between QCD and nucleon-nucleon (NN) forces. Several detailed reviews on the Skyrme model may be found in the literature (Holzwarth and Schwerdtfeger 1986, Zahed and Brown 1986, Schechter and Weigel 2000).

3.2. The Skyrme uid

For astrophysical applications, one needs a many-body description of the nuclear force, and for neutron star densities, an in-medium approach based on the relevant degrees of freedom in the theory. As a successful and theoretically sound model, the Skyrme Lagrangian bears further investigation as regards its application to astrophysics. A particularly useful mean-field model was developed in the work of Kalbmann (1997), who studied Skyrme ions in a dilute uid approximation, where auxiliary dilaton (ϕ) and vector (A) fields couple to the Skyrme ion and carry the

information of density and temperature. The (non-zero) expectation values of these background fields are determined from the Skym ion Lagrangian itself, in the spirit of the mean field approach.

The scale-invariant Lagrangian for the Skym ion model (augmented by the ;! fields) is given by

$$\begin{aligned} L &= L_2 + L_4 + L_m & V_B &= V + L_1 & (1) \\ &= e^2 \left(\frac{1}{2} \partial_0 \partial_0 - \frac{F^2}{16} \text{Tr}(L L) + \frac{1}{32e^2} \text{Tr}(L; L)^2 \right. \\ &\quad \left. + e^4 \frac{F^2 m^2}{8} \text{Tr}(U - 1) g! B - B \bar{U} + e^4 (4 - 1) \right] \\ &\quad + \frac{1}{4} (\partial_0 \partial_0 - \partial_0 \partial_0)^2 + \frac{1}{2} e^2 m^2 \partial_0 \partial_0; \end{aligned}$$

where

$$L = U^\mu \partial_\mu U : \quad (2)$$

In eqn.(1), F is the pion decay constant, e is the Skym ion parameter, and g_V is the πN coupling strength. Scale invariance is broken by quantum fluctuations of the QCD vacuum, and this feature is manifest since the dilaton mocks up the scale anomaly of QCD (Nielsen 1977, Collins et al, 1977)

$$T = \partial_\mu D = \frac{9}{8} g_s^2 G^a G^a \quad (3)$$

for massless quarks, where T is the trace of the energy-momentum tensor, $D = T^\mu_\mu$ is the dilatation current, g_s the strong coupling constant, and G^a the gluon field strength. From the above Lagrangian, it is easily verified that

$$T = (e_0 e)^4 : \quad (4)$$

In more familiar terms, $e_0^4 = 4B$, where B is the bag constant. The dilaton field also provides the required intermediate-range attraction in the $N N$ force. The π -meson couples to the baryonic (vector) current B and provides the right sign for the isospin-independent spin-orbit force. It can also stabilize the soliton in the absence of the Derrick term (L_4) (Adkins and Nappi 1984a). We have included a heretofore ignored pion mass term, which has recently shown to be important for multi-skym ion systems (Battye and Sutcliffe 2005). In fact, these authors find that alternate minima of the Skym ion energy functional can arise if either the baryon number or the pion mass is large. For the (physical) value of the pion mass, and the product ansatz for the Skym ions that we use in this work, we can continue to use the "hedgehog" ansatz²

$$U = \exp(i \vec{\alpha} \vec{F}(r)) ; \quad (5)$$

² The product ansatz is used for simplicity. For truly multi-skym ion shell-like solutions with large baryon numbers of 20 or more, the pion mass plays an important role.

with the Pauli matrices. In this case, the Skym ion mass is

$$\begin{aligned} M &= M_0 e^0; \quad M_0 = 4 \int^Z dr r^2 M_0(r); \\ M_0(r) &= \frac{F^2}{8} F^0 + \frac{2 \sin^2 F}{r^2} + \frac{\sin^2 F}{2e^2 r^2} \frac{\sin^2 F}{r^2} + 2F^0 \\ &\quad + \frac{m^2 F^2}{4} (1 - \cos F); \end{aligned} \quad (6)$$

where $e_0 = h_0$ and $!_0 = h_! 0$ henceforth denote mean-field values. The resemblance of the above form to the free Skym ion case comes from the association of with broken scale invariance. With the product ansatz for the Skym ion

$$U_{B=N}(r; R_1, \dots, R_N) = U(r - R_1) \dots U(r - R_N) \quad (7)$$

and the sum ansatz for the ;! fields

$$B_{B=N} = !_1 + \dots + !_N; \quad !_N = !_1 + \dots + !_N; \quad (8)$$

the mean-field treatment implies that the equations for the Skym ion uid may be derived by solving the Euler-Lagrange equations from L for a single free Skym ion in the absence of background fields, and rescaling as

$$r! e^0 r; \quad !! e^0 ! \quad (9)$$

in the presence of the medium (Kabermann 1997). The free Skym ion mass M_0 can be formally obtained by noting that the solution for $F(r)$ is (Adkins and Nappi 1984b)

$$F(r) = 0.759 \frac{e^m r}{r} : \quad (10)$$

The "effective mass" of the Skym ion in the uid is then $M = e^0 M_0$. We now have the tools to construct the equation of state for the Skym ion uid.

3.3. Equation of State

To obtain the equation of state, we require a relation between the pressure and energy density of the uid. In the mean-field approximation, the energy of N Skym ions per unit volume is given by

$$\begin{aligned} E_V &= 2g_N \int^Z \frac{d^3 p}{(2\pi)^3} E_p (n_p + n_{\bar{p}}) + V(e_0) \\ &\quad + \frac{1}{2} e^0 m^2 !_0^2 + g_V !_0 v; \end{aligned} \quad (11)$$

where $g_N = 1$ for pure neutron matter and $g_N = 2$ for symmetric matter. Here, the particle and anti-particle distribution functions are

$$n_p = \exp \frac{p}{T} + 1 \quad ; \quad n_{\bar{p}} = \exp \frac{p + \bar{p}}{T} + 1 \quad (12)$$

with the dispersion relations $p_p = E_p + g_V !_0$, $p_{\bar{p}} = E_{\bar{p}} - g_V !_0$, where $E_p = \sqrt{p^2 + M^2}$. The quantity E_p is related to the energy of an individual Skym ion E_{sk} by a Lorentz boost of the static solution (Kabermann 1997).

It implicitly includes a contribution from the pion mass term as

$$U_m = m^2 F^2 \int dr r^2 (1 - \cos F) : \quad (13)$$

The net (baryon-antibaryon) density is

$$v = 2g_N \int \frac{d^3 p}{(2\pi)^3} (n_p - n_{\bar{p}}) : \quad (14)$$

Since the scale of thermal excitations in the Skyrme uid is much less than the baryon chemical potential, we will work at $T = 0$ for this section.³ The Fermi distributions reduce to theta functions, and we may minimize the energy functional E_V to obtain the mean field values ϕ_0 and ϕ_1 . It also follows that the scalar density is

$$= \frac{g_N p_F^3}{3^2} ; \quad (15)$$

where p_F is the Fermi momentum of the baryon. The pressure of this ensemble is given by

$$P_V = \frac{2}{v} \frac{\partial (E_V = v)}{\partial v} : \quad (16)$$

Minimization of the energy eqn.(11) with respect to the ϕ_0 and ϕ_1 fields generates their respective equations of motion, which shows that the contribution of the vector meson ϕ_1 to the pressure grows with density and is positive, a consequence of acting in the repulsive channel. The dilaton gives a negative pressure and acts to bind the system. Its contribution to the effective mass is however, more complex, and is determined by the preservation of the trace anomaly in the model. These features are crucial in understanding the pressure-density and mass-radius relations that we obtain in the following section.

3.4. Fit parameters for symmetric nuclear matter

In order to reproduce nuclear matter phenomenology, four free parameters ($a_i, i = 1; 4$) are added to the conventional dilaton potential⁴. Then,

$$V = B [1 + e^4 (4 - 1)] + B [a_1 (e - 1) + a_2 (e - 1) + a_3 (e^2 - 1) + a_4 (e^3 - 1)] ; \quad (17)$$

with the "bag constant" $B = (240 \text{ MeV})^4$. Terms of the form e^n are the only ones that can be added to the potential in accordance with the anomaly condition

$$\frac{dV}{d} = 0 \quad (18)$$

³ While considering neutrino cooling, we naturally admit finite temperatures.

⁴ There is also the possibility of modifying the field potential (see Kalb et al. (1997) and references therein).

at $= 0$, implying $a_1 = a_2 + 2a_3 + 3a_4$.⁵ The parameters of the dilaton potential are constrained by demanding that at the saturation density of nuclear matter ($\rho_0 = 0.154 \text{ Baryons/fm}^3$) the properties of nuclear matter are recovered. We chose the effective mass $M = M_0 = 0.6$, the compressibility $K = 270 \text{ MeV}$, and a binding energy per nucleon $B_V = (M - E_V = v)$ of 16 MeV . On fitting to these properties, we find

$$a_1 = 1.699; \quad a_2 = 25.781; \quad (19)$$

$$a_3 = 29.237; \quad a_4 = 11.464 \quad (20)$$

and

$$g_V = 7.543; \quad (21)$$

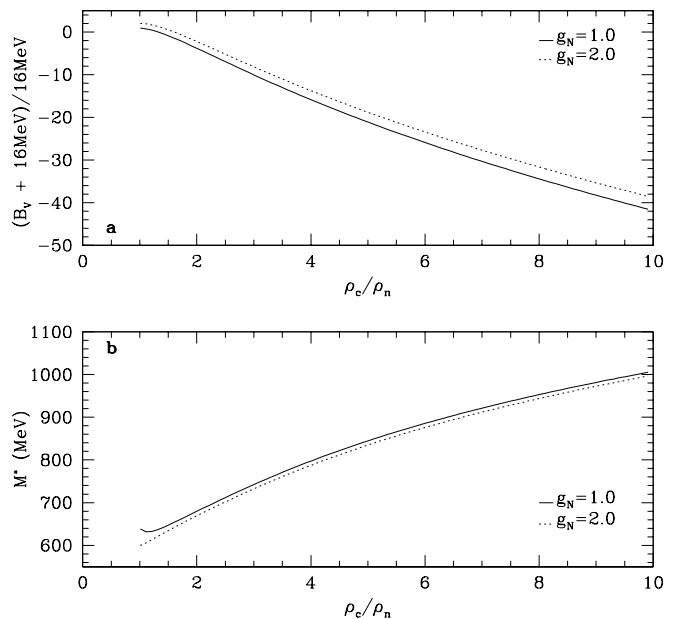


Fig.1. a). Binding energy per nucleon, as a function of the central density. The solid line is for pure neutron matter ($g_N = 1.0$) while the dotted line is for symmetric nuclear matter ($g_N = 2.0$). b). Effective Skyrme ion mass M (see eq.6) as a function of density.

Figure 1a shows the binding energy per nucleon as a function of the density while Figure 1b shows the Skyrme ion effective mass (M) as a function of density.

In the Waleck model – and many others similar to it – the nucleon mass decreases as a function of density. This is not the case in the Skyrme uid model. The minimum effective mass arises here at a density of around $1.2 \rho_0$ (for

⁵ One chooses the term multiplied by a_1 to have a negative power of e in order to avoid the introduction of a second minimum in the potential for $e = 0$. The only sensible minimum then remains the one at $e = 0$.

$g_N = 1.0$) and 1.0_0 (for $g_N = 2.0$). The reason for this difference can be traced back to the dynamics dictated by the dilaton, especially to the modified potential, as explained in Kalbemann (1997): The dilaton's attractive contribution to the mass is limited, since the solutions to nuclear matter exist only in a narrow region around $\phi = 0$, while the meson repulsion grows in direct proportion to the nuclear matter density. Beyond a certain density, tending to nuclear matter properties tends to push the dilaton towards positive values in order to fulfill the scaling properties of the model. The effective mass thus increases, and the quantity $(B_V + 16)$ (see Fig. 1a) actually decreases. These large qualitative differences from the usual class of

models stem from the unique form of the dilaton potential $V(\phi)$. This has important consequences on the type of compact objects constructed and brings us to the discussion of the stiffness of our EOS.

We now turn to applications of the Skyrme uid EOS. In the next section, we discuss the global structure of Skyrme stars and their cooling properties on the same footing.

4. Implications of the Skyrme EOS

4.1. Mass-radius relations

We proceed now to construct models for stars using the EOS developed above. This is done by integrating the general-relativistic equation of hydrostatic balance (Tolman 1934; Oppenheimer & Volko 1939) including rotation. For the rotating configurations we use the computer code RNS (Stergioulas & Friedman 1995; 1998). We specify the equation of state and the central energy density, and the code computes models with increasing angular velocity until the star is spinning with the same angular velocity as a particle orbiting the star at its equator (see Ouyed 2002).

Figures 2a and 2b show the resulting stellar masses and radii as a function of the central density, respectively. The masses are in the range $0.4 \leq M \leq 3.45$ while the radii (equatorial circumferential radius; proper equatorial circumference/2) are calculated to be $18.6 \text{ km} \leq R \leq 23.0 \text{ km}$. In Figure 2c, we show the resulting Mass-Radius plane. Note that the maximum mass configuration does not correspond to the maximum radius case. In general, for a given central density, rotation allows the masses and radii to increase by 30% and 40%, respectively, when compared with the non-rotating cases. The amount of mass in the outer region of the star (the crust region - $\phi < \phi_N$ - constructed using the EOS of Baym, Pethick & Sutherland, 1971) decreases with rotation (see Figure 3). The crust of rotating Skyrme stars constitutes less than 5% of the total mass while it averages 20% for the static configurations. The minimum spin period for Skyrme stars was computed to be $0.8 \text{ ms} \leq P \leq 2.0 \text{ ms}$ (Ouyed 2002).

A comparison of the mass-radius curve for the Skyrme star with that of neutron and quark stars (see Figure 4)

shows a qualitative difference that arises from the physics of the dilaton discussed previously. The limited attractive force provided by the dilaton leads to large stiffness even at moderate central pressures when compared to ordinary neutron stars. The radius of Skyrme stars increases with mass within a certain region, despite increased gravitational forces, similar to the curve for self-bound quark stars. Although Skyrme stars are also bound by gravitational forces, they do not display a 'hill' as do neutron stars.

4.2. Neutrino cooling of the Skyrme uid

A unique method to probe the internal composition of a neutron star is by tracing its temperature evolution with cooling simulations (Pethick 1992, Page 1998, Yakovlev et al. 2003). Neutron stars are born in supernova explosions and as the neutron star cools, neutrinos begin to free stream and essentially leave the star without further interaction. As a consequence, about 30 seconds after the explosion, the cooling of neutron stars is controlled by neutrino emission. Importantly, the neutron stars remain luminous enough during the neutrino cooling era, so that the surface temperature can be extracted from space telescope data and the theoretical cooling curves can be confronted with observations. There is a host of well-known neutrino emission processes that operate in the crust and core of the neutron star (Yakovlev et al. 2001), and which one dominates the cooling depends mainly on the temperature and to a lesser extent, on the density. Since cooling rates are dependent on neutrino emissivities, which in turn depend on the dense matter equation of state employed, it is instructive to compute the dominant neutrino emission rates. We now proceed to do so for the Skyrme uid. We address only the global thermal energy balance of the star during the neutrino cooling era, so that we may employ

$$C_V \frac{dT}{dt} = -L \quad (22)$$

to compute the cooling history. The required inputs to the above equation are the total specific heat at constant volume C_V and the neutrino emissivity Q which determines the neutrino luminosity $L = Q V$, where V is the cooling volume of the star. The main neutrino emission process in our case is neutrino bremsstrahlung from neutron-neutron collisions⁶. At tree level, the neutrino emissivity can be determined from the set of Feynman diagrams shown in Figure 5.

The calculation proceeds in a manner analogous to that described in Friedman & Maxwell (1979), who worked in neutron matter with a phenomenological description of nuclear forces, and explicit nucleon fields. In our case, we use the Skyrme model, which can reproduce the long-range part of the $N\bar{N}$ interaction, namely, the one-pion

⁶ In the absence of any charged species, this is indeed the dominant neutrino emission process. Inclusion of the more powerful modified Urca process requires extending the model used here to asymmetric matter.

exchange (Nyman & Riska 1990).⁷ The interaction between the nucleons is then given by

$$V(k) = \frac{g_{NN}}{4m} \frac{2}{k^2 + m^2} \frac{^{(1)}\mathbf{k} \cdot \mathbf{k}^{(2)}}{^{(1)}\mathbf{k}^2 + m^2} \cdot \cdot \cdot ; \quad (23)$$

where $g_{NN} = 11.9$ ⁸ is the pion-nucleon coupling constant and $m = 138$ MeV. The superscripts on the spin and isospin operators indicate the two nucleons. Although we have used a relativistic model for the nucleons thus far, we approximate their dispersion relations by their non-relativistic counterparts for calculational simplicity. Thus, $E_p = p^2 = 2M$, $p^4 = 8M^3 + \dots$. The relative error in retaining only the leading term is about $p_F^2 = 4M^2 = 10\%$ if we consider densities as high as 2_{N} . This will not affect our final result for the emissivity in any considerable way. At higher densities, the Fermi momentum of the nucleon is not small compared to its effective mass M , and a fully relativistic treatment is required. Here, we restrict our application to Skym ion stars with central densities $\rho_c = 2_{\text{N}}$ so that our non-relativistic approximations hold. From the plots of mass versus central density and mass versus radius, we observe that this limits us to $M = 2M$ and $R = 15$ km. Thus, we are well within current observational limits.

The emissivity is given by

$$Q = N \sum_{i=1}^Z \frac{Y^4}{(2^i)^3} \frac{d^3 p_i}{2!_1 (2^i)^3} \frac{d^3 Q_1}{2!_2 (2^i)^3} \frac{d^3 Q_2}{2!_2 (2^i)^3} \cdot \cdot \cdot \quad (24)$$

$$(2^i)^4 (E_f - E_i)^3 (P_f - P_i) \frac{1}{s} \frac{X}{\text{spin}} M_{\text{nn}} \cdot \cdot \cdot$$

$$! F(E_{p_i});$$

where p_i denote the momenta of the incoming and outgoing neutrons and $Q_{1,2} = (!_{1,2}; Q_{1,2})$ label the neutrino energies and momenta. The delta functions account for energy and momentum conservation, and $! = !_1 + !_2$ is the total neutrino energy. N denotes the number of neutrino species and $s = 2$ is a symmetry factor for the initial neutrons, when the emission occurs in the final state or vice versa. The function $F(E_{p_i}) = f(E_{p_1}) f(E_{p_2}) (1 - f(E_{p_3})) (1 - f(E_{p_4}))$ is the product of Fermi-Dirac distribution functions $f(E_p) = (\exp((E_p - T) + 1)^{-1}$. The matrix element M_{nn} includes the nucleon-nucleon scattering part derived from the potential $V(k)$ and the coupling to the emitted neutrino pair. Neutrino pair emission from a neutron line is given by the neutral current V . A weak interaction

$$L_{\text{weak}}^n = \frac{G_F}{2^i 2} \frac{Y}{2} (!_0 - g_A)_{i,i} \cdot \cdot \cdot \quad (25)$$

⁷ Short-range interactions were considered in Friman & Maxwell (1979), and were found to compensate the effect of the inclusion of exchange diagrams (§ 4). Therefore, we only retain the direct contributions in the computation.

⁸ This is the predicted value in the model (Adkins and Neppi 1984b) that we are using, compared to the actual experimental value of 13.2. The model parameters are chosen to reproduce the nucleon (938.9 MeV) and Delta (1232 MeV) mass.

with Fermi coupling constant $G_F = 1.166 \cdot 10^5$ GeV², the neutrino current $l = u(Q_1) (1 \cdot 5) u(Q_2)$, the non-relativistic nucleon spinors denoted by u and $u(Q_{1,2})$ the relativistic spinors for the neutrinos, which are taken to be massless. The weak axial-vector coupling constant $g_A = 0.65$. The value of g_A obtained in this model is about half the experimental value, but this is related to the fact that the Skym ion model result derives from a large N_c approximation, and for $N_c = 3$, an additional multiplicative factor of $5/3$ must be introduced, bringing g_A to 1.08, closer to the experimental number of 1.26, which may be quenched to 1 in dense nuclear/neutron matter. Thus, this is not a shortcoming of the model, per se. We take $g_A = 0.65$ to be consistent with the other model parameters that we use. Furthermore, the behavior of the axial form factor as a function of momentum transfer q^2 in the Skym ion model deviates significantly from the experimentally measured dipole parameterization even at low q^2 (Braaten et al. 1986). However, since the scale of q^2 is set by thermal excitations, and $T = p_F$, we use the value $g_A(q^2 = 0)$.

The final result for the emissivity in analytical and numerical form is (in natural units $h = c = 1$ and $k_B = 1$)

$$Q = \frac{41}{14175} \frac{G_F^2 g_A^2 M^4 p_F^4}{(2^i)^5} \frac{g_{NN}}{2m} \frac{4}{F} \frac{m}{2p_F} T_9^8; \quad (26)$$

$$F(x) = 1 - \frac{3}{2} x \tan^{-1} \frac{1}{x} + \frac{1}{2} \frac{x^2}{1+x^2} \cdot \cdot \cdot \quad (27)$$

$$Q = 3.75 \cdot 10^8 \frac{M}{N} \frac{4}{M_0} T_9^8$$

$$F = \frac{205}{(\frac{M}{N})^{1/3}} \text{ erg cm}^{-3} \text{ s}^{-1}; \quad (28)$$

where we have included three flavors of neutrino. The quantity M is related to the effective mass as

$$\frac{1}{M} = \frac{1}{M} + \frac{2g_V}{p_F^2} !_0 \quad (29)$$

and is therefore a function of density. A plot of the emissivity as a function of temperature T_9 for two different densities $\rho = \rho_{\text{N}}$ and $\rho = 2_{\text{N}}$ is shown in Figure 6.

The neutrino luminosity L is now determined as

$$L = 4 \int_0^{R_b} dr r^2 Q(r); \quad (30)$$

where R_b denotes the distance from the center of the star to the bottom of the crust. The specific heat of the baryons can be expressed as

$$c_V = 2 \frac{d^3 p}{(2^i)^3} (!_p - \frac{\partial f}{\partial T}); \quad (31)$$

where we have omitted a term that is negligible in the degenerate limit. In this limit, one can extract the density of

states $D(F)$ at the Fermi surface and express the specific heat as

$$C_V = D(F) \frac{2T}{3} = \frac{1}{3} T p_F \text{eff}; \quad \text{eff} = \frac{q}{p_F^2 + M^2} : \quad (32)$$

In numerical terms, with the relations $M = 0.6M_0$ and $p_F = 336(=N)^{1/3}$,

$$C_V = 9.76 \cdot 10^0 T_9 \frac{1}{N} \frac{q}{s} \frac{1}{0.355} + 1 \text{ erg cm}^{-3} \text{ K}^{-1} : \quad (33)$$

The total specific heat is then

$$C_V = 4 \int_0^{R_b} dr r^2 C_V(r) : \quad (34)$$

With eqns.(30) and (34), we can now proceed to compute the cooling curve for the uid region of the star. In fact, an analytical estimate is easily made (Page et al 2004). Performing the integrations in eqns.(30) and (34), we obtain

$$L = N T^8; \quad C_V = C T : \quad (35)$$

The cooling equation (22) can then be integrated to yield

$$T = \frac{C}{6N} t^{1/6} \quad (36)$$

for long-term cooling in the neutrino dominated epoch. The "internal" temperature T is the temperature at the bottom of the crust, and can be related to the effective temperature at the surface of the crust via the so-called Tsuruta law (Tsuruta 1979) which is an interpolation between the surface and the crust temperatures. The formula for thick crusts as is the case in our model is (see also Shapiro & Teukolsky 1983, p330) $T_s = (10T_m)^{2/3}$; the subscript "m" stands for mantle.

The effective temperature as seen by a distant observer is then $T_e^1 = T_e \frac{1}{R_{\text{Sch}}} = R$ where R_{Sch} is the star's Schwarzschild radius. The resulting cooling curve is plotted in Figure 7 for Skym ion stars with central density $c = 2N$. The cooling curves for the non-rotating configurations correspond to $M = 2.2M_0$; $R = 16$ km and those for the maximally rotating ones correspond to $M = 3.0M_0$; $R = 22$ km. The two initial temperatures chosen essentially bracket the temperature data on young and moderately old neutron stars. Note that we included photon cooling which starts to dominate when $L_e = L_s$. In that era, the T vs. t behavior is (Page et al. 2004)

$$T = \frac{C}{4S} t^{1/4} \quad (37)$$

where C is the same constant as before, $S = 0.05$, and

$$S = 4.4 \cdot 10^{6.6} R_{10}^2 g_s \text{ ergs}^{-\text{sec}} \text{ K}^{2.4} ; \quad (38)$$

$$g_s = 1.33 \frac{M}{M} \frac{e^s}{R_{10}^2} ; \quad (39)$$

$$s = \frac{1}{1 + 0.3 \frac{M}{M} \frac{1}{R_{10}}} \quad (40)$$

with R_{10} the stellar radius in units of 10 km. The photon luminosity is given by $L = ST^{2.4}$. We observe that photon cooling starts to dominate close to a million years after the neutron star's formation. The exceedingly rapid cooling of the star then makes it truly invisible.

5. Conclusion

In this work, we have examined the case for considering the Skym ion model as a viable description of dense nuclear matter, with direct application to neutron star interiors. There are clear indications that conventional neutron matter equations of state cannot explain the observation of some very heavy neutron stars, unless the central densities are assumed to be fairly high. The Skym ion Lagrangian, within the mean-field approach employed here, and with the inclusion of the dilaton, serves to generate quite stiff equations of state that can describe the structure of these heavy stars. Importantly, the Skym ion model incorporates features of QCD such as scale breaking (the trace anomaly) and chiral fields that map to low-lying excitations of the vacuum. It should be noted, however, that the use of the dilaton as an interpolating field to mimic the (large) scale-breaking in QCD appears at odds with the estimated glueball mass of 1.5 GeV and its stiffness in matter (Birse (1994)). A better medium description of the Skym ion model would have to take this fact into consideration.

To be consistent with the treatment of cooling, we have included the effects of a finite pion mass in the model. While this introduces some changes in the analytic expressions for the pressure and energy, the overall mass-radius relations are not affected from the massless case because the change in the t parameters is very small (less than 1%). At higher densities than those considered here, it is possible that the inclusion of a physical pion mass causes distortion in the skym ion profile. The mass-radius curves for Skym ion stars are distinct from ordinary neutron stars, essentially due to the qualitatively different nature of the dilaton potential, which respects the scale anomaly, and is related to nuclear matter properties. We have described both rotating and non-rotating configurations for Skym ion stars, the essential difference between them being the crustal mass fraction, and the total mass that they can support (rotating configurations can support considerably more mass). Skym ion stars can be useful in describing observations of large mass neutron stars. Such stars are indirectly hinted at in astrophysical

models of the r-process, cooling curves of neutron stars, and have been examined in population synthesis studies.

We have also studied cooling of Skymion stars with a crust by identifying the dominant neutrino emission process, and computing the corresponding emissivity. A long with the specific heat of degenerate matter, this allows us to sketch the cooling history of the star from hundreds of years (when the star becomes isothermal) up to a million years when the star rapidly cools to unobservably low temperatures. A more accurate cooling curve can be produced by taking into account the thermal conductivity of the material. This allows us to study heat diffusion and the early cooling period of the star. We have included the effects of a thick crust, described by the BPS equation of state, as well as photon cooling, assuming a generic envelope at the surface. While these surface structures are not direct consequences of our model, they are "pinned on" here for a more realistic picture, and to enable qualitative comparisons to the neutron star temperature data. We have not included the effects of superfluidity (pairing gaps) on neutrino emission and cooling, which can close certain neutrino production channels, and open others. These are known to play an important role in the thermal evolution of the star, and affect the inference of stellar masses from the cooling curve. The underprediction of g_A and g_{NN} in the model implies that the neutrino emissivity is also underestimated by a factor 5. However, this has only a slight effect on the cooling rate since the temperature depends on the 1/6th power of the ratio C/N (see eqn.(36)).

An additional contribution to the neutrino flux that we have ignored in this work comes from the electroweak decay of charged pions to neutrinos. Furthermore, neutral pions can also decay into neutrino-antineutrino pairs. Although this process is forbidden by helicity conservation in vacuum, the presence of a medium implies that decay can occur in a frame moving with respect to the preferred rest frame. In fact, this process has been addressed within the Skymion model very recently (Kalloniatis et al 2005). The reason we have neglected such "pionic" contributions is that the corresponding neutrino rate is penalized by an exponential factor of $\exp(-m/T)$. Since $T \ll m$ in our case, the neutrino emissivity is exponentially small. The dominant contribution in our model is indeed from the Bremsstrahlung process.

Assuming a mean-field approach to the Skymion uid and ignoring Skymion overlap at high density is no doubt a simplification, but our aim in this work has been to gauge the model's main features, and examine its potential for the astrophysics of neutron stars. While improvements can surely be made on the theoretical and numerical aspects of the assumed model, we find that it displays qualitative features regarding its mass-radius curve that are very different from ordinary neutron stars. This could bear importantly upon the observations of heavier mass neutron stars as well as their cooling history.

Acknowledgements. P.J. thanks the Department of Physics and Astronomy at the University of Calgary, where this work was initiated, for its hospitality. The research of R.O. is supported by grants from the Natural Science and Engineering Research Council of Canada (NSERC) as well as the Alberta Ingenuity Fund (AIF). P.J. is supported by the Department of Energy, Office of Nuclear Physics, contract nos. W-31-109-ENG-38 and DE-FG02-00ER41135.

References

Adkins, G. S. and Nappi, C. R. 1984a, Physics Letters B 137 no. 3, 251

Adkins, G. S. and Nappi, C. R. 1984b, Nucl. Phys. B 233, 109

Battye, R. A. and Sutcliffe, P. M. 2005, Nucl. Phys. B 705, 384

Baym, G., Pethick, C. J. and Sutherland, P. 1971, ApJ. 170, 299

Birse, M. C. 1994, J. Phys. G 20, 1287

Braaten, E., Tse, S. M. and Wilcox, C. 1986, Phys. Rev. D 34, 1482

Clark, J. S., Goodwin, S. P., Crowther, P. A. et al. 2002, A & A 392, 909

Collins, J., Duncan, D. and Joglekar, S. D. 1977, Phys. Rev. D 16, 438

Friman, B. and Maxwell, O. V. 1979, ApJ 232, 541

Gendenning, N. K. 1997, Compact Stars (Springer, New York)

Haensel, P. 2003 in 'Final Stages of Stellar Evolution', EAS Vol 7, J.-M. Hameray and C. M. O'Ceallaigh editors, EAS Publications Series

Heiselberg, H. 2001, in Proceedings of the conference on Compact Stars in the QCD Phase Diagram, R. Ouyed and F. Sannino editors, NORDITA, Copenhagen, Denmark

Heiselberg, H. and Pandharipande, V. 2000, Ann. Rev. Nucl. Part. Sci. 50, 481

Holzwarth, G. and Schwesinger, B. 1986, Rep. Prog. Phys. 49, 825

Kalbermann, G. 1997, Nucl. Phys. A 612, 359

Kalloniatis, A. C., Carroll, J. D. and Park, B.-Y. 2005, astro-ph/0501117

Kaminker, A. D., Haensel, P., and Yakovlev, D. G. 2001, A & A 373, L17

Lattimer, J. M. and Prakash, M. 2001, ApJ 550, 426

Lattimer, J. M. and Prakash, M. 2004, Science Vol. 304, 536

Lattimer, J. M. and Prakash, M. 2000, Phys. Rep. 333, 121

Li, X.-D., Ray, S., Dey, J., Dey, M., & Bombaci, I. 1999, ApJ 527, L51

Manchester, R. N. 2004, Science 304, 542

Nice, D. J., Splaver, E. M., and Stairs, I. H. in IAU Symposium 218, ASP Conference Proceedings, F. Camilo and B. M. Gaensler editors

Nice, D. J., Splaver, E. M., and Stairs, I. H. 2004, to appear in "Binary Radio Pulsars", F. A. Rasio & I. H. Stairs editors, PASP conf series; [astro-ph/0411207]

Nielsen, N. K. 1977, Nucl. Phys. B 120, 212

Nyman, E. M. and Risika, D. O. 1990, Rep. Prog. Phys. 53, 137

Otsuki, K., Tagoshi, H., Kajino, T., and Wanajo, S. 2000, ApJ 533, 424

Oppenheimer, J. R., and Volkov, G. M. 1939, Phys. Rev. 55, 373

Ouyed, R. and Butler, M. 1999, ApJ 522, 453

Ouyed, R. 2002, A & A 382, 939

Page, D. P., Lattimer, J. M., Prakash, M. and Steiner, A. W. 2004, to appear in ApJ supplements; [astro-ph/0403657]

Page, D. P. 1998 in 'The Many Faces of Neutron Stars', Proceedings of the NATO Advanced Study Institute, R. Buccieri, J. van Paradijs and M. A. Alpar editors, Kluwer

Pethick, C. J. 1992, Rev. Mod. Phys. 64, 133

Popov, S. B., and Prokhorov, M. E. 2005 [astro-ph/0412327]

Quaintrell, H., Norton, A. J., Ash, T. D. C. et al. 2003, A & A 401, 313

Ransom, S. R., Hessels, J. W. T., Stairs, I. H., Freire, P. C. C., Camilo, F., Kaspi, V. M. and Kaplan, D. 2005, Science Vol. 307, Issue 5711, 892

Schechter, J. and Weigel, H., review article published in INSA - Book-2000

Schwenk, A. 2004, talk at 12th International Conference on Recent Progress in Many-Body Theories, Santa Fe.

Schwenk, A., Friman, B. and Brown, G. E. 2003, Nucl. Phys. A 713, 191

Skym, T. H. R. 1962, Proc. R. Soc. London A 260, 127

Shahbaz, T., Casares, J., Watson, C. et al. 2004, ApJ 616, L123-126

Shapiro, S. L. and Teukolsky, S. A. 1983, Black Holes, White Dwarfs and Neutron Stars, John Wiley & Sons, Inc. N.Y.

Stergioulas, N. and Friedman, J. L. 1995, ApJ 444, 306

Stergioulas, N. and Friedman, J. L. 1998, ApJ 492, 301

Sumiyoshi, K., Suzuki, K., Otsuki, K., Terasawa, M. and Yamada, S. 2000, Publ. Astron. Soc. Japan 52, 60

't Hooft, G. 1974, Nucl. Phys. B 72, 461

Thorsett, S. E. and Chakrabarty, D. 1999, ApJ 512, 288

Tolman, R. C. 1934, Proc. Natl. Acad. Sci. 20, 169

Tsuruta, S. 1979, Phys. Rep. 56, 237

van Kerwijk, M. H. 2001, in Proceedings of the Jan van Paradijs Memorial Symposium, E. P. J. Van den Heuvel, L. Kaper and E. Roleditors (ASP, San Francisco)

Waber, F. 1999, Acta Phys. Polon. B 30, 3149

Witten, E. 1979, Nucl. Phys. B 160, 57

Witten, E. 1983a, Nucl. Phys. B 223, 422

Witten, E. 1983b, Nucl. Phys. B 223, 443

Witten, E. 1984, Phys. Rev. D 30, 272

Yakovlev, D. G., Gnedin, O. Y., Kaminker, A. D., Levensh, K. P. and Potekhin, A. Y. 2003, Adv. Space Res. 33, 523

Yakovlev, D. G., Kaminker, A. D., Gnedin, O. Y. and Haensel, P. 2001, Phys. Rept. 354, 1

Zahed, I. and Brown, G. E. 1986, Phys. Rep. 142, 1

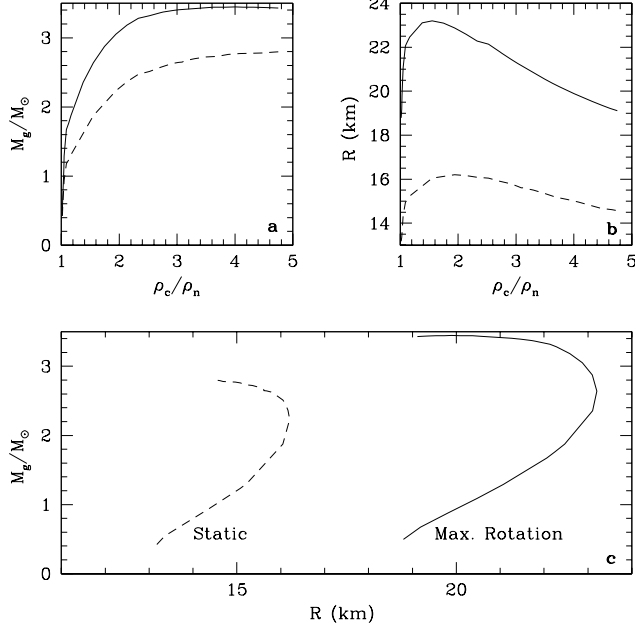


Fig.2. a). Gravitational mass versus central density for zero temperature Skym ion stars in hydrostatic equilibrium. In this figure, the solid curves represent the rotating configurations while the dashed curves represent the non-rotating or static configurations. b). Radius versus central density for Skym ion stars in hydrostatic equilibrium. c). The Mass - Radius plane. Note that only the $g_f = 1$ case is shown.

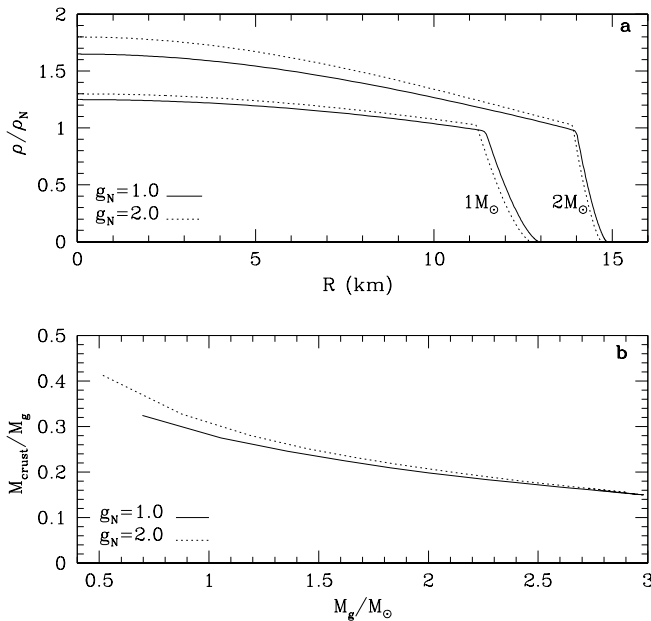


Fig.3. a). Density profiles for 1M and 2M static models of Skym ion stars. b). The crustal mass fraction: the crust is defined as the subnuclear region where the EOS of BPS has been adopted.

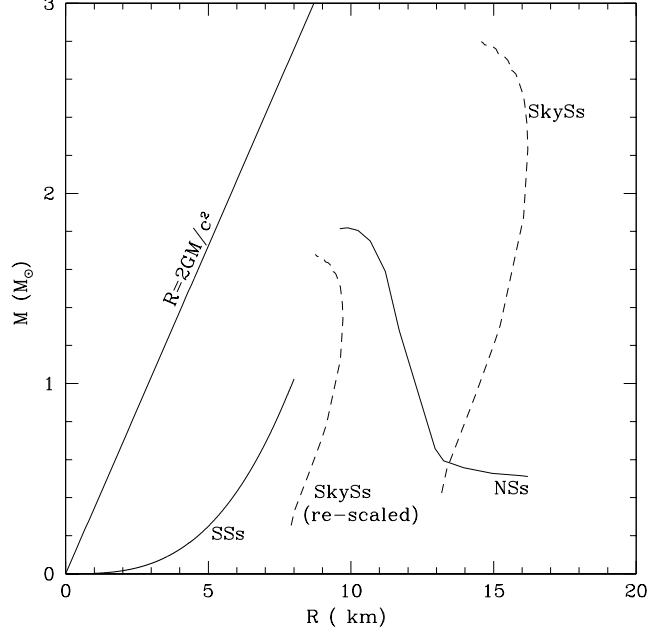


Fig.4. Mass-Radius relationship characteristic of neutron stars (NSs; e.g. G lendenning 1997) and quark stars (SSs; e.g. Li et al. 1999) as compared to Skym ion stars (SkySSs). The SkySSs models have been re-scaled for better comparison.

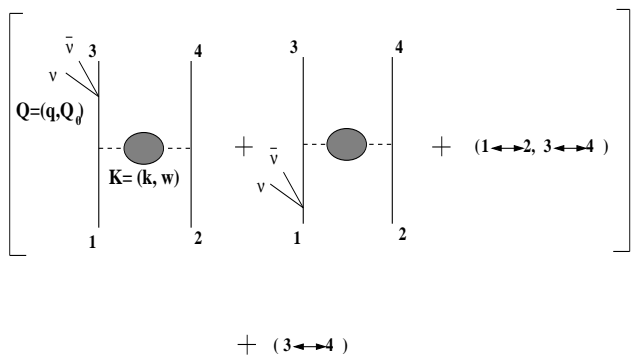


Fig.5. The Feynman diagrams for neutrino bremsstrahlung in neutron-neutron collisions. The first 4 diagrams, enclosed within square brackets, are the "direct" contributions while the interchange (3 \leftrightarrow 4) generates the exchange diagrams. The blob represents one-pion exchange (see text for details).

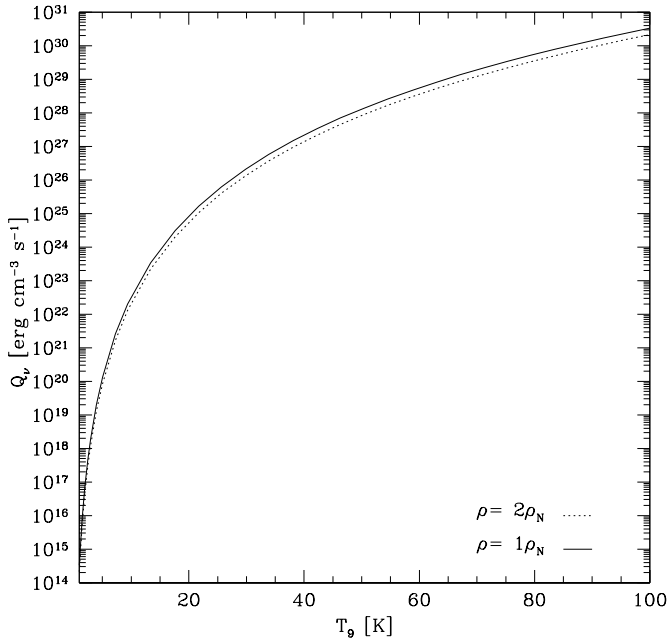


Fig.6. Neutrino emissivity (Q_ν) as a function of temperature T_9 for two different densities $\rho = \rho_N$ (solid line) and $\rho = 2\rho_N$ (dotted line).

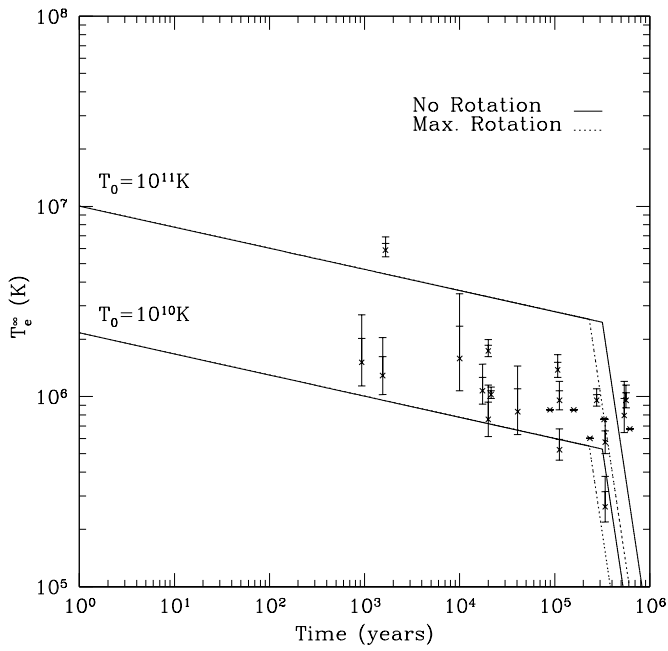


Fig.7. Cooling curve for Skym ion stars with central density $\rho = 2\rho_N$, for maximally rotating (dashed) and static (solid) configurations.